

VIBRATION-INDUCED DROPLET ATOMIZATION

M. K. Smith, A. James, B. Vukasinovic, and A. Glezer
The George W. Woodruff School of Mechanical Engineering
Georgia Institute of Technology, Atlanta, GA 30332-0405
marc.smith@me.gatech

INTRODUCTION

Thermal management is critical to a number of technologies used in a microgravity environment and in Earth-based systems. Examples include electronic cooling, power generation systems, metal forming and extrusion, and HVAC (heating, venting, and air conditioning) systems. One technique that can deliver the large heat fluxes required for many of these technologies is two-phase heat transfer. This type of heat transfer is seen in the boiling or evaporation of a liquid and in the condensation of a vapor. Such processes provide very large heat fluxes with small temperature differences. A heat pipe is an example of a device that exploits such two-phase heat transfer to provide high heat fluxes in a simple passive device. However, one of the limitations of the heat pipe is that the heat flux is limited by the rate at which the liquid phase is transported along the pipe by the capillary wicking material.

The purpose of our work is to improve on the passive heat pipe by using a more active means of transporting the liquid phase in a similar heat transfer cell. The process we are considering is called vibration-induced droplet atomization. In this process, a small liquid droplet is placed on a thin metal diaphragm that is made to vibrate by an attached piezoelectric transducer. The vibration induces capillary waves on the free surface of the droplet that grow in amplitude and then begin to eject small secondary droplets from the wave crests. In some situations, this ejection process can develop so rapidly that the entire droplet seems to burst into a small cloud of atomized droplets that move away from the diaphragm at speeds of up to 50 cm/s. If such a process could be incorporated into a heat transfer cell, the active atomization and transport of the small liquid droplets could provide a much larger heat flux capability for the device.

The first step in exploiting this bursting process for use in heat transfer cells or in any other technology is to understand the basic atomization process itself. In the sections that follow, we present some of our work on the nature and character of this phenomenon. First, we discuss in more detail the nature of a typical bursting event. Then, we describe the experimental apparatus and protocols used in this research and

present data that characterizes the bursting process in this system. The response of the system can be explained in terms of a simple interaction between the droplet ejection process and the nonlinear dynamics of the vibrating diaphragm. This interaction is embodied in a simple mathematical model that is described next. Finally, we discuss the results, present our conclusions, and describe our future work with this process.

DROPLET BURSTING

The overall phenomenon of droplet bursting is shown in Figure 1. A liquid droplet with a volume of approximately 200 μl and a diameter of approximately 5 mm was placed at the center of a horizontal, circular metal diaphragm. The diaphragm was clamped at its periphery and was driven by a piezoelectric ceramic disk centrally-mounted on its bottom side. Excitation of the piezoelectric disk caused the diaphragm to

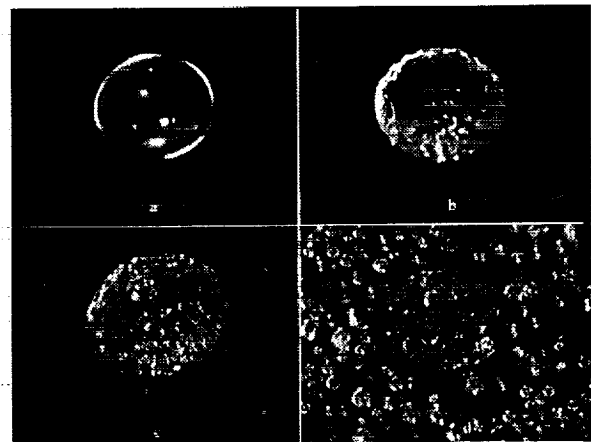


Figure 1: A sequence of video frames showing perspective views of a liquid droplet on a vibrating diaphragm. The excitation frequency is held fixed. The excitation amplitude is increased from image a) to c) and then fixed after that. a) The undisturbed droplet, b) non-axisymmetric wave motion on the surface, c) intense wave motions over the entire droplet surface and the ejection of a few small secondary droplets, and d) the small secondary droplets that have fallen on the diaphragm after the bursting event.

vibrate in the vertical direction in its fundamental axisymmetric mode. Figure 1 shows a sequence of video frames of this system as the excitation amplitude is increased, but with the frequency fixed at about 1000 Hz. Figure 1a shows the unforced droplet for reference. For small values of the excitation amplitude, axisymmetric standing waves appeared on the surface of the droplet. At slightly higher excitation amplitudes, the droplet underwent a transition to a non-axisymmetric wave form as shown in Figure 1b. The excitation amplitude was increased once again and in Figure 1c, we see that the surface waves have increased in magnitude and complexity and that a few small secondary droplets have already been ejected from some of the wave crests. At this point, we held the excitation amplitude fixed and observed a slow intensification of the droplet ejection process until suddenly, within a half a second or so, the entire droplet seemed to explode into a spray of much smaller secondary droplets. The spray was directed away from the surface of the diaphragm with initial droplet ejection speeds of up to 50 cm/s. The ejected droplets reached a maximum height above the diaphragm of about 5 cm. The end result of this bursting process is shown in Figure 1d, where we see that most of the ejected secondary droplets have landed back on the surface of the diaphragm under gravity.

The bursting process displayed in Figure 1 has several interesting fluid dynamical events. The first is the appearance of the standing axisymmetric waves on the free surface of the droplet. These waves are classical Faraday waves with some edge modifications due to the contact line of the droplet. The instability of these waves produces the non-axisymmetric motions that were observed. Such instabilities have been reviewed by Miles and Henderson (1990).

The Faraday waves grow in amplitude and complexity as the driving amplitude is increased until we begin to see the ejection of a few small secondary droplets from the wave crests of the primary droplet. This kind of droplet ejection has been studied by several other researchers in related geometries (see Goodridge, et al., 1996 for example). While the rate of droplet ejection depends on the excitation amplitude, the more interesting fact is that for a fixed excitation amplitude the rate of ejection slowly increases with time. At this point in the process, the wave motion seems to have become more evenly distributed across the free surface of the primary droplet and the droplet ejection sites seem to occur evenly throughout the center portion of the droplet.

The most interesting event is the burst. It occurs after the first appearance of droplet ejection and the

length of time needed to burst depends on the excitation amplitude. When a large excitation signal is applied to the diaphragm, bursting can occur immediately. For smaller excitation amplitudes (but still large enough), bursting may be delayed on the order of seconds to maybe a minute or more after the forcing is applied.

The purpose of this paper is to describe and characterize this dramatic bursting event. In the sections that follow, we describe our experiments and mathematical modeling of the bursting process and present some results.

EXPERIMENTAL SETUP

The experimental apparatus used in this work is shown in Figure 2. The transducer used to vibrate the liquid droplet was a circular steel diaphragm 29 mm in diameter and 0.2 mm thick. A piezoelectric ceramic was plated onto a small circular area centered on the lower surface of the diaphragm. The diaphragm was mounted in an aluminum ring holder by clamping the outer edge with a retaining ring. The inside diameter of this ring and thus the active diameter of the vibrating diaphragm was 27 mm. The diaphragm was excited using a signal generator coupled to an amplifier that applied a constant sinusoidal voltage to the ceramic. This causes the ceramic to expand and contract, which in turn induces the diaphragm to vibrate in its fundamental axisymmetric mode. The frequency and voltage applied to the ceramic were monitored and controlled.

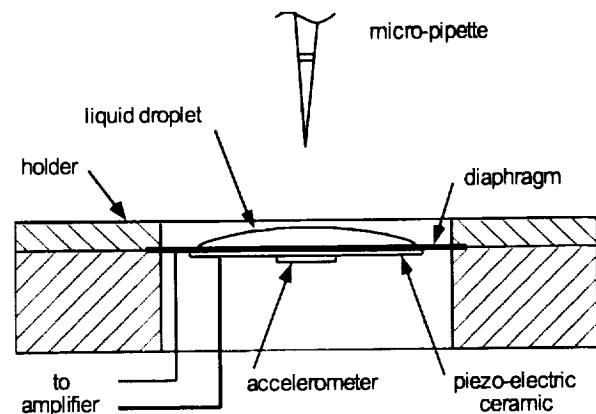


Figure 2: A sketch of the experimental setup.

The acceleration of the diaphragm was measured with a small accelerometer glued to the center of the piezoelectric ceramic on the lower surface of the diaphragm. The accelerometer has a range of 350 g

and a precision of about ± 0.01 g. Given a nominal forcing frequency of 1000 Hz, we only recorded the oscillation amplitude of the output from the accelerometer. This amplitude was obtained with a small circuit that squared the voltage signal from the accelerometer and then passed it through a 40 Hz low-pass filter. The resulting signal was sampled at a rate of 100 Hz. A square root was taken once the signal was discretized by the data acquisition computer.

Finally, the temperature of the aluminum retaining ring was monitored by an embedded thermocouple in order to correct the final results for variations in the temperature of the diaphragm due to the small but normal variations in the ambient temperature of the room.

The upper surface of the diaphragm was cleaned prior to each run using a strict protocol. This was done in order to reduce any possible contamination of the free surface of the droplet so as to promote the repeatability of the results. At the very beginning of each set of runs, an air duster was used to remove any microscopic dust that might have been present on the diaphragm. The cleaning procedure before each run consisted of the following steps: removal of the secondary droplets from the previous run using a small pipette, drying of the surface by tissue, surface cleaning by acetone, and finally, cleaning by distilled water.

We used distilled water in these experiments. Varying volumes of water ranging from 100 μ l to 400 μ l were placed at the center of the upper surface of the diaphragm using a micro-pipette with a precision of about 1 μ l. The free surface motion on the droplet and the evolution of the bursting event were recorded using a video camera with a 1/10,000 sec shutter speed.

A typical response plot of the acceleration amplitude of a dry diaphragm versus frequency for various values of the applied voltage is shown in Figure 3. The symbols are the experimental data points and the solid curves are the results of the mathematical model that we shall describe later. The behavior of this system is typical of a slightly nonlinear structural system forced near its resonance frequency. The influence of a small droplet of water (without any droplet ejection) on this behavior is shown in Figure 4. For these data, we set the driving amplitude well below the amplitude needed for any droplet ejection to occur. We see that the additional mass of the water droplet lowers the resonance frequency of the system as expected. In addition, the peak acceleration amplitude at resonance decreases slightly as the frequency decreases. This behavior is

typical of the structural damping that occurs as a result of the flexing of the steel diaphragm.

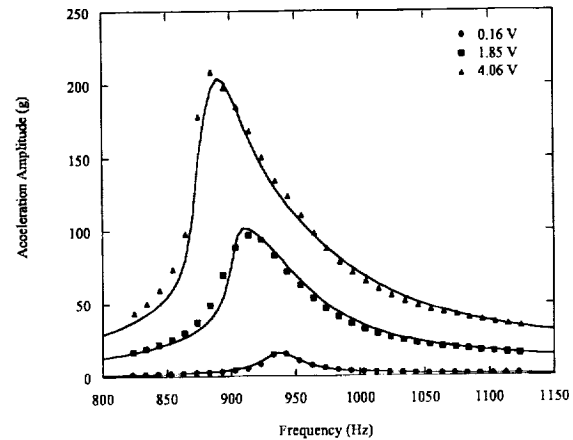


Figure 3: The frequency response of a dry diaphragm for various values of the applied voltage (measured in volts). The acceleration is measured in units of one gravity.

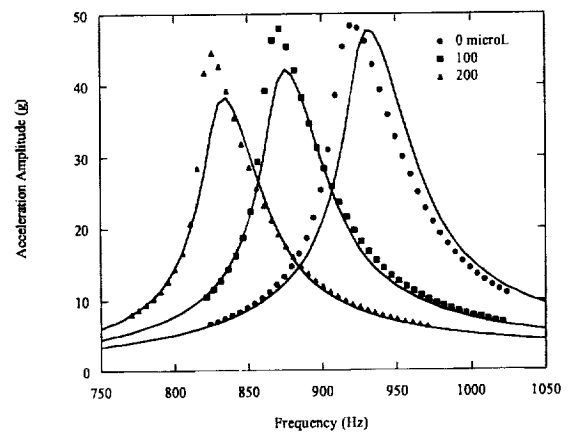


Figure 4: The effect of the droplet mass on the frequency response of the diaphragm for two different droplet volumes (measured in microliters). The acceleration is measured in units of one gravity.

Figure 5 shows the acceleration amplitude of a typical bursting event in our experiment. For these experiments, a constant voltage is applied to the diaphragm at time zero. Initially, the acceleration of the diaphragm jumps to a value corresponding to the imposed voltage. It then slowly increases from this initial value. During this time we observed a few

small droplets being ejected from the large droplet and land back on the diaphragm. Then suddenly, the acceleration rapidly rises to a maximum and decreases to a new, but lower constant level. The rapid change in acceleration occurred when the droplet was observed to burst. For a driving frequency closer to the initial resonance frequency of the system or for a higher driving voltage the bursting signature can be made to occur almost immediately. We shall discuss this event in more detail in the following section.

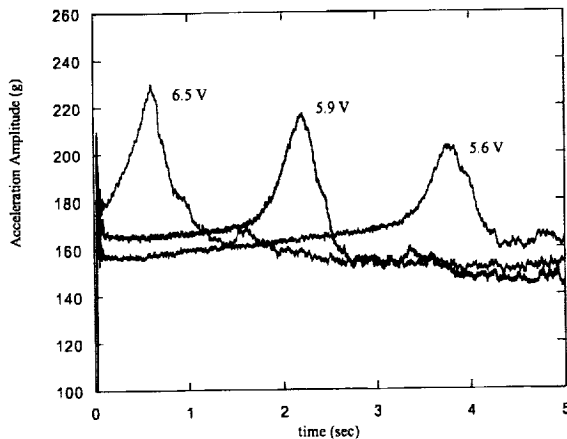


Figure 5: The acceleration signature of a bursting droplet for various driving voltages and at a driving frequency of 750 Hz.

MATHEMATICAL MODEL

Our mathematical model of the diaphragm-droplet system is shown in Figure 6. The diaphragm is modeled as a lumped mass connected to a nonlinear spring, a nonlinear structural damper, and a piezoelectric driving element. We account for the axisymmetric motion of the diaphragm by using the generalized mass of the diaphragm and the piezoelectric ceramic based on the measured mode shape in this frequency range. The stiffness of the diaphragm is included using a nonlinear spring function fitted to the observed behavior of the diaphragm without any water droplets present. Also based on our observations, a small amount of structural damping is included. The piezoelectric element is simply a linear spring that can vary its own length x when a voltage is applied. The droplet is also modeled as a lumped mass. We account for the initial spreading of the droplet by computing a generalized mass for a droplet with a given volume, a given

contact angle, and a spherical-cap shape using the same mode shape of the diaphragm as before. We account for droplet ejection by allowing the droplet mass to decrease at a linear rate if the acceleration of the diaphragm is large enough.

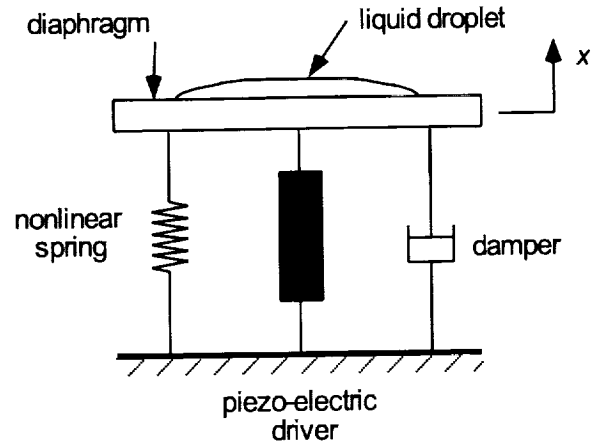


Figure 6: The mathematical model of the diaphragm and liquid droplet system.

In this one-degree-of-freedom model, the motion of the diaphragm is described by the following pair of differential equation in time:

$$m\ddot{x} + \frac{c(x)}{\omega}\dot{x} + k(x)x = A \cos(\omega t) \quad (1)$$

$$m = f(m_d, m_r) \quad (2)$$

$$\dot{m}_d = \begin{cases} 0, & \ddot{x} < a_c \\ -r(\ddot{x} - a_c), & \ddot{x} > a_c \end{cases} \quad (3)$$

Here, x is the displacement at the center of the diaphragm and m is the total generalized mass of the system. It is composed of m_d , the generalized mass of the diaphragm, m_r the residual mass of the droplets that have fallen back on the diaphragm. The structural damping of the system is $c(x)$, $k(x)$ is the nonlinear spring function for the system, A is the driving coefficient derived from the piezoelectric element, and ω is the frequency of the oscillations. Finally, r is the rate of droplet ejection from the large primary droplet and a_c is the critical acceleration above which droplet ejection occurs.

These two equations were integrated in time using the fourth-order Runge-Kutta integrator in MATLAB (ode45). To compare the numerical results to the experimental data, the acceleration time response was squared and digitally low-pass-filtered with the same

cutoff frequency of 40 Hz as in the experiments. The results were then square-rooted and plotted. To give the best comparison to the experimental data, the nonlinear functions for the stiffness and the structural damping of the diaphragm were fitted to the data for a dry diaphragm. The two parameters characterizing the bursting process, r and α_c were fitted to the data in order to produce the best overall agreement between the model and the experiments.

RESULTS

The first results of our simulations, plotted in Figure 3, show good agreement between the model and the experiment. This simple model does a good job of predicting the behavior of the dry diaphragm over a range of driving voltages because the model parameters were optimized for these conditions. Nevertheless, the results show that this simple model of a lumped spring-mass-damper system is a good one for this apparatus.

The effect of adding a droplet to the diaphragm is shown in Figure 4. As mentioned earlier, the droplet mass lowers the resonance frequency and amplitude of the system. We track the drop in the resonance frequency quite well, but over-predict the drop in the peak resonance amplitude. We are about 14% lower than the experimental peak at the largest droplet volume considered. The discrepancy is primarily due to the fact that the structural parameters for the model were optimized for a system acceleration response of about 100 g. The experimental data in Figure 4 have a peak acceleration no larger than 50 g.

A simulation of droplet bursting is shown in Figure 7. This is a plot of the acceleration of the diaphragm versus time for several different driving voltages. The 5.9 V level is the threshold voltage. Below this value, no secondary droplets are ejected from the primary droplet. For larger driving voltages, we see a relatively slow increase in the acceleration amplitude on the plate until suddenly the voltage rises and falls to a slightly lower level.

While the quantitative agreement between the bursting results of the experiment and the simulations shown in Figure 5 and Figure 7 are not very good, at least the general trends are predicted. We see that as the driving voltage increases, the ejection time peak is shifted to smaller times, the peak response increases slightly, and the final response is slightly reduced. The differences are primarily due to the simplicity of the mathematical model used for both the droplet ejection process and the vibration of the diaphragm.

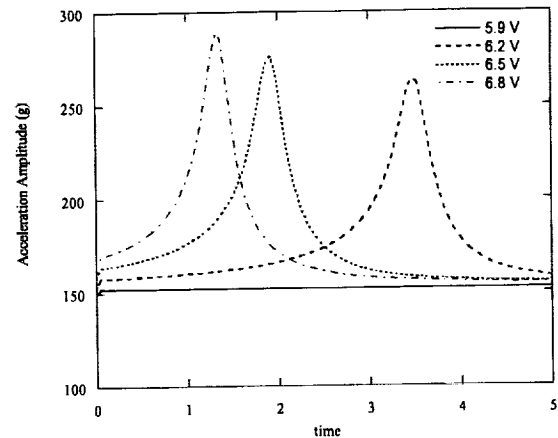


Figure 7: The numerical simulation of the acceleration signature of a bursting droplet driven at 825 Hz. The acceleration is measured in units of one gravity.

CONCLUSIONS

An analysis of the experiments and simulations presented above show that a droplet bursting event occurs when the system passes through a resonance condition. To explain this process, assume the fact that small secondary droplets are ejected from the crests of free surface waves on the larger droplet when the acceleration amplitude of the diaphragm is larger than a critical value. Also, assume that the rate of droplet ejection depends on the magnitude of this acceleration. Bursting occurs when the initial acceleration of the diaphragm is higher than the critical acceleration and the driving frequency is larger than the initial resonance frequency of the diaphragm-droplet system. Under these conditions, some droplet ejection occurs immediately after the driving voltage is applied. If the initial diaphragm acceleration is too high, the rate of droplet ejection will be very large and the droplet will appear to burst immediately.

If the initial diaphragm acceleration is just above the critical acceleration, the rate of droplet ejection from the larger droplet will be very small. As the secondary droplets are ejected, the effective mass of the diaphragm-droplet system is reduced, which increases the resonance frequency of the system and brings it closer to the driving frequency. When this occurs, the vibration amplitude of the system increases, leading to even more droplet ejection. In this way, the droplet ejection process allows the system to pass through its resonance frequency and to experience the very large peak acceleration associated

with this event. If this peak acceleration is large enough, it will drive the droplet ejection rate to the large values needed to produce a bursting event.

The time delay for the bursting event depends on the difference between the initial diaphragm acceleration and the critical acceleration. The smaller this difference, the larger the time delay for bursting to occur. Also, if the initial driving frequency is below the resonance frequency of the system, bursting may not occur at all. If the initial driving acceleration is just large enough to cause a low rate of droplet ejection, the system will then move away from resonance, the acceleration of the diaphragm will decrease, and droplet ejection will slow down and it may stop completely.

The key to the droplet atomization process we have investigated is the piezoelectric vibrating diaphragm. This simple device gives us an easy and consistent way to achieve accelerations above 200 g, which are needed to atomize and eject the small secondary droplets from larger droplets or films. The device is inexpensive and its power requirement is very small. In contrast, traditional shakers that attain these levels of acceleration are very large, expensive, and difficult to use.

We have incorporated this device into a design for a new heat transfer cell for use in a micro-gravity environment. The cell is essentially a cylindrical container with a hot surface on one end and a cold surface on the other. The vibrating diaphragm is mounted in the center of the cold surface. Water droplets condense on the cold surface and collect on the vibrating diaphragm. Here, they are atomized and propelled against the hot surface, where they evaporate. The water vapor travels back across the cell and condenses on the cold surface, where the cycle is repeated. A prototype of this heat transfer cell has been built and tested. It can operate continuously and provides a modest level of heat transfer, about 20 W/cm². Our work during the next few years will be to optimize the design of this cell to see if we can produce a device that has significantly better performance than conventional heat exchangers and heat pipes.

Finally, we have begun a series of experiments and numerical studies that will give us a detailed understanding of the process through which droplets are ejected from a free surface wave crest. We need this information in order to determine the critical acceleration and the rate of droplet ejection used in our simple vibration system model described above. This level of understanding of the droplet ejection process will allow us to optimize the vibration induced droplet atomization technology for use in such things

as our heat transfer cell in a microgravity environment. In addition, it will allow us to adapt the technology for use in other processes or systems, such as spray coating, emulsification, encapsulation, etc. In addition, we may be able to devise new ways to do things that are now done by other, possibly less efficient methods.

ACKNOWLEDGMENTS

This work was supported by the NASA Microgravity Research Division through grant number NAG3-1949.

REFERENCES

- Goodridge, C. L., Shi, W. T., and Lathrop, D. P. (1996) "Threshold Dynamics of Singular Gravity-Capillary Waves," *Phys. Rev. Lett.* **76**, pp. 1824-27.
- Miles, J. & Henderson, D. (1990) "Parametrically Forced Surface Waves," *Ann. Rev. Fluid Mech.* **22**, pp. 143-65.